

HIGH EFFICIENCIES ON MC-SI SOLAR CELLS ENABLED BY INDUSTRIAL FIRING THROUGH REAR SIDE PASSIVATING SiN_x:H

I.G. Romijn, M. Koppes, E.J. Kossen, C.J.J. Tool, A.W. Weeber
ECN Solar Energy, P.O. Box 1, 1755 ZG Petten, The Netherlands
Phone: +31 224 564309; Fax: +31 224 568214; email: romijn@ecn.nl

ABSTRACT: A current challenge in developing low-cost mc-silicon solar cells is to substitute the aluminum back surface field (BSF) to allow the use of much thinner wafers. To be able to reach higher efficiencies on thin wafers the rear surface passivation, the internal rear side reflection and the cell bowing ask for better rear side properties than those of the now commonly used Al BSF. In this paper we present our first steps toward a solar cell of the future that will overcome these drawbacks. We will demonstrate that silicon nitride (SiN_x) can be implemented in an industrial cell line as a rear surface passivating layer reaching higher efficiencies compared to an Al BSF, and without bowing. The rear contacts can be directly fired through the SiN_x, without the need to open the layer. Efficiencies up to 15.5% were reached on mc-Si wafers with rear surface recombination velocities ($S_{\text{eff, rear}}$) down to 175 cm/s. This low $S_{\text{eff, rear}}$ will not be limiting the efficiency up to at least 17% cell efficiency. Moreover, up to these efficiencies the good rear side passivation is not hindered by parasitic shunts (caused by fixed charges in the silicon nitride).

Keywords: Cell processing, multi crystalline, silicon nitride, passivation, recombination

1 INTRODUCTION

Reaching high efficiencies on thin and large solar cells is one of the best ways to reduce costs of multi crystalline silicon (mc-Si) PV technology. To be able to reach these higher efficiencies on thin wafers, the existing solar cell concepts with aluminium back surface field (BSF) have to be adjusted. The increased importance of recombination losses at the surfaces (figure 1), lower internal rear side reflection and the increased cell bowing of thinner wafers, ask for a better rear side quality than that of an Al BSF. In this paper, we present our first steps towards a solar cell of the future (figure 2).

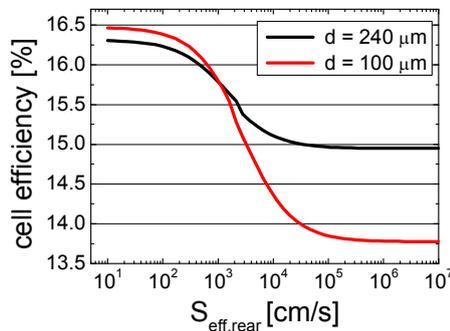


Figure 1: Efficiencies of solar cells with different thicknesses for a range of rear surface recombination velocities (S_{rear}). For thinner cells ($\sim 100 \mu\text{m}$), this recombination velocity becomes increasingly important, giving a large reduction in efficiency for $S_{\text{rear}} > 800 \text{ cm/s}$. For $S_{\text{rear}} \leq 200 \text{ cm/s}$ the efficiency remains stable.

We will demonstrate that silicon nitride (SiN_x) coatings can be used as a rear surface passivating layer and implemented in the standard industrial mc Si solar cell lines with a simple firing-through process. No grinding [1], lasering [2] or etching [3] was used to open the rear surface SiN_x layer.

It is often argued [4,5] that the performance of SiN_x layers on the rear side of p-type solar cells will be inadequate, due to parasitic shunts caused by a high amount of fixed charges. We show that solar cells with the metallic contacts isolated from the rear side SiN_x layer give the same rear-IQE and J_{sc} , and thus have the

same effective rear side passivation, as cells where these contacts are not isolated.

Efficiencies up to 15.5% were reached on mc-Si wafers, while even higher efficiencies will be possible upon increasing the Fill Factor. We show that with SiN_x on the rear side of p-type mc-Si solar cells an $S_{\text{eff, rear}}$ down to 175 cm/s can be reached on cells where the Al contacts are fired through the SiN_x. These values are better than those of our Aluminium BSFs, and good enough to reach 17% on lower material quality with the ECN advanced inline cell processing [6], especially on thinner wafers. This means that silicon nitride as rear surface passivating layers will not be the limiting factor for high efficiency mc-Si solar cells!

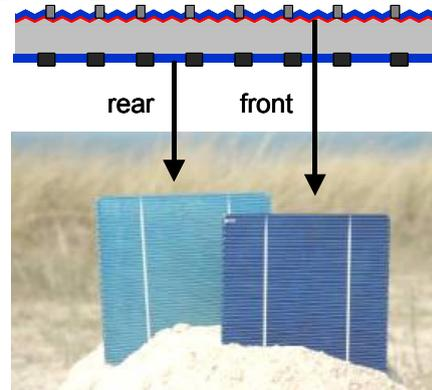


Figure 2: A solar cell of the future: silicon nitride passivating layer on both front and rear side, texture on front and polished surface on the rear side.

2 EXPERIMENTAL

2.1 Optimizing surface passivating coatings

Several different SiN_x and SiO_x layers were tested for their rear surface passivating qualities, while also the preparation of the surface of the wafers before deposition was investigated. All test layers were deposited on both sides of double side polished FZ wafers, and their effective lifetime (τ_{eff}) was measured using the Quasi Steady State Photo Conductance method [7]. Subsequently, S_{eff} was calculated using $1/\tau_{\text{eff}} = 1/\tau_{\text{bulk}} + S/2W$, with $\tau_{\text{bulk}} = 1\text{ms}$.

The thermal stability of the passivating layers was investigated by measuring the lifetime before and after an anneal comparable to that of firing the metallization.

The silicon nitride coatings were deposited with our remote MW PECVD system, using NH_3 and SiH_4 as precursor gasses, and were all around 80 nm thick. The silicon oxide layers were grown in a tube furnace at 900 °C, to thicknesses of 7 and 15 nm. On top of these oxides an 80nm thick silicon nitride layer was deposited for protection and stabilization of the passivation.

2.2 Solar cells

270 μm p-type mc-Si and 240 μm Cz wafers were processed using the sequence shown in figure 2. The effect of rear side polishing on the surface passivation was compared to leaving the surface textured (arrow in figure 3). An H pattern Al metallization was used for rear side contacting and local BSF formation. Both the Ag front and Al rear contacts were fired through the SiN_x -H layers in a single co-firing step. Only step 4 and 6 (red) are added to the standard cell processing.

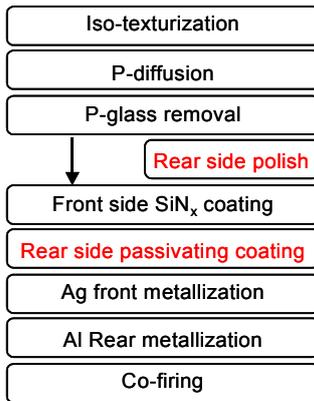


Figure 3: Flow chart of processing of rear side passivated solar cells

The cell results were analysed in detail by current-voltage (IV) and internal quantum efficiency (IQE) measurements. The IQE was taken from both the front and the open rear side of the solar cells. By fitting both front and rear IQE in PC-1D with the same parameters for τ_{bulk} and S_{rear} , accurate knowledge on the rear surface passivation could be obtained [8,9]. These analyses and simulations were also used to identify further improvements, and the effect of the thickness on the cell efficiency.

3 RESULTS AND DISCUSSION

3.1 Recombination velocities on FZ test samples

In figure 4 recombination velocities (S_{eff}) of several types of silicon oxide and silicon nitride on the FZ wafers are shown. The recombination velocities of the $\text{SiO}_x/\text{SiN}_x$ stack layer 2, and of SiN_x layers 5 to 7, remained below 40 cm/s even after firing. SiN_x layer 4 is the ECN baseline coating, used for all front sides of the solar cells in the experiments.

In the following experiments, both nitride layer 7, a layer specially dedicated to rear side passivation, and the best oxide layer (2) were tested on the rear side of mc-Si solar cells. Although the silicon nitride shows better passivation on FZ wafers, the silicon oxide might perform better on solar cells due to the fewer amount of

fixed positive charges [4,5].

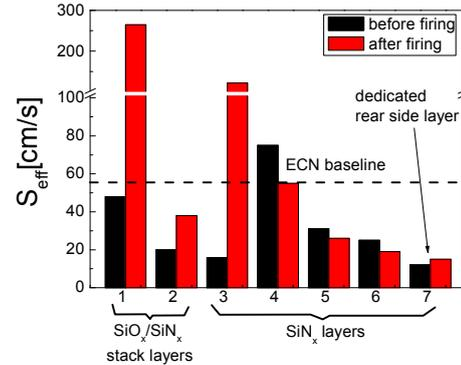


Figure 4: Recombination velocities of different silicon oxide and silicon nitride coatings, before and after firing. The ECN Baseline SiN_x layer (4) is used for the front side of the solar cells. SiN_x layer (7) was especially optimized for rear side coatings.

3.2 Implementation of rear surface passivation in solar cells.

In table I the results of mc-Si and Cz-Si solar cells using different rear surface pre-treatments and rear surface coatings are summarized.

The rear side passivating properties are obtained from PC-1D analysis of IQE measurements from both the front and rear side of the solar cells: The bulk lifetime of the wafers, τ_{bulk} , can be determined with the IQE measured from the front for wavelengths between 800 – 1000 nm, and with the IQE measured from the rear around 1000 nm. Similarly, $S_{\text{eff, rear}}$ can be 'fitted' using the IQE measured from the front between 900 to 1000 nm and the IQE measured from the rear between 600 to 1000 nm. For lower wavelengths the results of the IQE measured from the rear are affected by the absorption in the passivating layers. Thus, when fitting the solar cells with PC-1D, both front and rear side IQE can be used simultaneously and fitted with one parameter set. Except for the full Al rear surface cells, the IQE measurements from the rear side of the solar cells with different rear side passivation schemes are shown in figure 5, including the fits from the PC-1D analysis.

Table I: Improvement on rear surface passivation

Wafer type	Rear side	J_{SC} (mA/cm ²)	V_{OC} (mV)	S_{eff} (cm/s)	FF (%)	η (%)
mc-Si	Full Al	33.5	610	300	75.5	15.4
	No passivation	31.9	591	2*10 ⁵	60	11.3
	SiO _x	32.2	599	2200	62	11.9
	SiN _x	32.8	603	600	67	13.2
	Polished + SiN _x	33.4	606	425	77.2	15.5
mc-Si	Optimized rear	34.1	604	175	73.1 / 77	15.1 / 15.8
Cz Si	Polished + SiN _x	33.8	609	500	76	15.7

The first three groups of solar cells (no passivation, $\text{SiO}_x/\text{SiN}_x$ stack and SiN_x on the rear side) were made without additional polishing of the rear side. Going from no rear surface passivation to a rear surface SiO_x layer capped with a 80 nm thick SiN_x layer, S_{eff} decreases from

10^5 cm/s to 2200 cm/s, with a corresponding increase in both J_{sc} and V_{oc} . Applying the best passivating layer, rear side dedicated silicon nitride, $S_{eff, rear}$ becomes even lower, 600 cm/s. Although we did not reach the very low $S_{eff, rear}$ that were found on the FZ test samples, also here the silicon nitride layer performed better than the silicon oxide layer. A higher $S_{eff, rear}$ on the solar cells compared to the FZ test samples is expected since the additional handling and (industrial) process steps will influence the surface conditions. Moreover, the rear surfaces of these solar cells were not yet polished. The decrease in rear side recombination velocity from $S_{eff, rear} = 2200$ cm/s to 600 cm/s is easily seen from the rear-IQE graph, and is reflected in an increase in current of almost 2%, and an increase in V_{oc} of 0.7% (see table I). For these cells the FF was still lower since the firing through the SiN_x on the rear was not fully optimized yet.

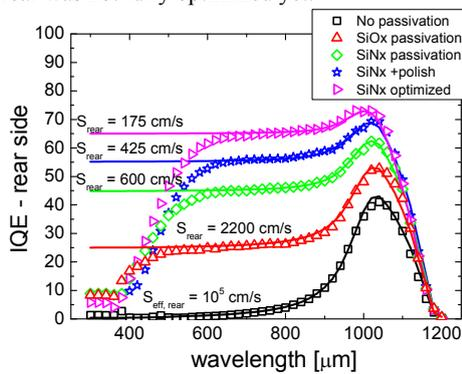


Figure 5: IQE measurements and PC1d fits from the rear side of the solar cells

Including a rear side polishing step prior to depositing the silicon nitride layers, the rear surface passivation increases with a corresponding decrease in $S_{eff, rear}$ to 425 cm/s, reaching values below those that are usually achieved with industrial Al BSFs. For this group, J_{sc} obtained with SiN_x rear side passivation is comparable (33.4 vs 33.5 mA/cm²), while the V_{oc} is only 0.7% less (606 vs 610 mV) than the corresponding group with full Al BSF. Due to a higher FF (77.2%), however, the cells with a SiN_x rear have a 0.1% absolute higher efficiency. On Cz wafers efficiencies of 15.7% were reached with this processing.

The best rear surface passivation was obtained after optimizing our rear surface treatment and polishing. Recombination velocities below 200 cm/s were reached, better than those with our reference Al BSF. As can be seen from figure 6, the front side IQE of the open cell is similar from 800-1000 nm, and higher at wavelengths > 1000 nm than that of the full Al solar cell. This increase at wavelengths > 1000 nm is due to a high rear side reflection caused partly by the measurement chuck. When mounted into a module this higher reflectivity will be realized by the rear side foil. The current rises correspondingly to 34.1 mA/cm². Optimizing the firing (FF=77%) would lead to cell efficiencies of about 15.8%.

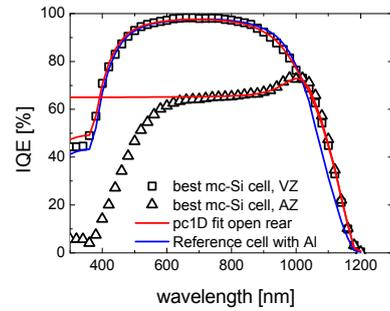


Figure 6: IQE and PC-1D fits from the rear and front of the best solar cell with SiN_x rear surface passivation. The IQE from the full Al reference is also shown

3.3 Parasitic shunts?

Although the values reached for rear side recombination velocities < 200 cm/s are very good and give no indication of a reduction due to fixed charges, this possibility investigated [4,5]. To investigate the possible reduction in rear side passivation due to parasitic shunts, on some cells the rear side silicon nitride was locally opened before metallization. The metallization was applied in such a way that it was either isolated from the passivating layer (see figure 7), or overlapping with the silicon nitride.

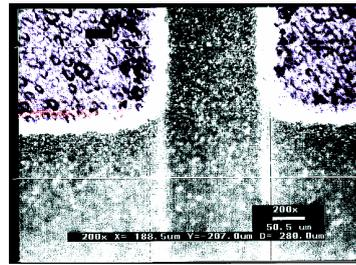


Figure 7: microscope photo of metallization (gray) printed inside an opened pattern (white) in the silicon nitride (bluish).

As can be seen from the rear side IQE graphs in figure 8, there is no difference in the rear side passivation between cells with metallization isolated from the rear surface SiN_x layer and those cells with contacts fired through the silicon nitride. Neither was there any difference seen in J_{sc} (both J_{sc} averaged 33.7 mA/cm²). This means that, at least down to $S_{rear} = 200$ cm/s (the fitted value for these cells), there is no influence of parasitic shunts on the rear surface passivation.

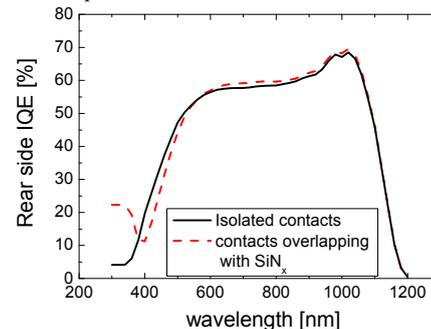


Figure 8: Rear-IQE from cells with isolated metallic contacts (black line) and with metallization overlapping with SiN_x (red line). The response is the same, showing that there is no decrease in rear surface passivation due to parasitic shunts.

3.4 Future high efficiency processing

In a recent publication Tool et al. reported record efficiencies on industrially inline processed mc-Si solar cells of 17% [6]. This ECN high efficiency processing involved advanced texturization (additional 3% gain in J_{sc}), high ohmic shallow emitter diffusion ($74 \Omega/\square$) and full surface Al BSF on good mc-Si materials (giving $\tau_{bulk} > 90 \mu s$). In table II PC-1D fits of this high efficiency inline processed cell are shown together with those from our new rear side processing.

The parameters fitted with PC-1D on the 15.5% cell and on the best rear passivated cell ($S_{eff, rear} = 175 \text{ cm/s}$) are shown in the first two columns. Again, the very high reflection found for cells with a SiN_x rear side coating is caused by the additional reflection of the measurement chuck. When mounted into a module this higher reflectivity will be realized by the rear side foil. In the third column, the PC-1D fitted parameters of the 'Barcelona top cell' are shown. In column 4 and 5, the advanced texturization and high ohmic emitter processing are combined with the open rear side processing, on both lower quality material and on higher quality material.

As can be seen from the PC-1D simulations and from figure 9, using the ECN advanced front side processing we will be able to obtain efficiencies of 17%, equal to those of our best ECN mc-Si cell, with an open rear side on lower quality material. When the material thickness decreases, efficiencies of the open rear side solar cell will increase (green line in figure 9) while those of the 'Barcelona top cell' (black line in figure 9) will decrease. This decrease in efficiency for thinner cells is mainly caused by the lower reflection of the Al BSF.

Finally, using high quality material, efficiencies up to 17.5% could thus be obtained with open rear side solar cells! Furthermore, it can be seen that the expected efficiency for cells thinner than $150 \mu m$ will be less dependent on the material quality when a $\text{SiN}_x\text{:H}$ passivated rear side is applied.

Table II: parameters found in PC1d fits of the IQE and IV data, and the improvements that can be made

	Best cell				
parameter	Polished rear	Improved rear	Barcelona top cell	Top, open rear	Top, open rear
				Low τ	High τ
	PC1d fit	PC1d fit	PC1D fit	calculate	calculate
Thickness (μm)	270	270	300	270	270
Emitter Ω/\square	67	67	74	74	74
τ_{eff} (μs)	30	30	90	30	90
S_{front} (cm/s)	$7 \cdot 10^5$	$5 \cdot 10^5$	$2 \cdot 10^5$	$2 \cdot 10^5$	$2 \cdot 10^5$
S_{rear} (cm/s)	425	175	350	175	175
R_{rear} (%)	87	87	67	87	87
V_{oc} (mV)	606	604	624	619	626
J_{sc} (mA/cm 2)	33.4	34.1	35.4	35.6	36.4
FF (%)	77.2	77	77	77	77
η (%)	15.5	15.8	17.0	17.0	17.5

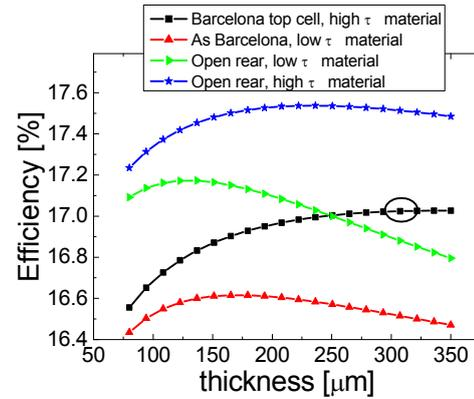


Figure 9: Efficiency of several types of solar cells as a function of wafer thickness, calculated from the PC1D fitted parameters from table II. The 'Barcelona top cell' has a full Al BSF and is compared to two solar cells with advanced front side processing and SiN_x passivated rear side.

4 CONCLUSIONS

We developed an inline industrial process using firing through a passivating SiN_x at the rear side. No grinding, lasering or etching was used to open the rear surface SiN_x layer. All processes can be easily transferred and implemented into an industrial solar cell line. Efficiencies equal to the reference process using full Al-BSF have been reached. Lowest S_{eff} reached is better than that of an Al BSF. This means that silicon nitrides as rear surface passivating layer will not be the limiting factor for high efficiency mc-Si solar cells made on thin and large wafers! Optimized integration in the advanced ECN inline process will make efficiencies of 17% or higher possible.

5 ACKNOWLEDGEMENTS

This work was financially supported by the FP6 European Crystal Clear project (EC contract SES6-CT-2003-502583) and by Senter Novem.

6 REFERENCES

- [1] A. Metz and R. Hezel. Proc. 28th IEEE Photovoltaic Specialists Conference, Anchorage, September 2000
- [2] E. Schneiderlöchner et al., Proc. 19th EU PVSEC, Paris, June 2004
- [3] G. Agostinelli et al., Proc. 20th EU PVSEC, Barcelona, June 2005
- [4] S. Dauwe, L. Mittelstädt, A. Metz, R. Hezel, Progress in Photovoltaics, Res. And Appl., 10, 271-278, 2002
- [5] O. Schultz et al., Proc. Proceedings WCPEC-4 Hawaii 2006.
- [6] C.J.J. Tool et al., Proc. 20th EU PVSEC, Barcelona, June 2005
- [7] R. A. Sinton, A. Cuevas, Appl. Phys. Lett 69, 2510 (1996)
- [8] P.A. Basore, D.A. Clugston, PC-1D v5.5, University New South Wales 2000.
- [9] M. Rinio et al., Proc. Proceedings WCPEC-4 Hawaii 2006.